Available online at www.sciencedirect.com
SCIENCE DIRECT®

Icarus 164 (2003) 254–259

ICARUS

www.elsevier.com/locate/icarus

The mass ratio of Charon to Pluto from Hubble Space Telescope astrometry with the fine guidance sensors ☆

C.B. Olkin,* L.H. Wasserman, and O.G. Franz

Lowell Observatory, 1400 West Mars Hill Road, Flagstaff, AZ 86001-4499, USA

Received 3 July 2002; revised 20 March 2003

Abstract

The mass ratio of Charon to Pluto is a basic parameter describing the binary system and is necessary for determining the individual masses and densities of these two bodies. Previous measurements of the mass ratio have been made, but the solutions differ significantly (Null et al., 1993; Young et al., 1994; Null and Owen, 1996; Foust et al., 1997; Tholen and Buie, 1997). We present the first observations of Pluto and Charon with a well-calibrated astrometric instrument—the fine guidance sensors on the Hubble Space Telescope. We observed the motion of Pluto and Charon about the system barycenter over 4.4 days (69% of an orbital period) and determined the mass ratio to be 0.122 ± 0.008 which implies a density of 1.8 to 2.1 $\mathrm{g\,cm^{-3}}$ for Pluto and 1.6 to 1.8 $\mathrm{g\,cm^{-3}}$ for Charon. The resulting rock-mass fractions for Pluto and Charon are higher than expected for bodies formed in the outer solar nebula, possibly indicating significant postaccretion loss of volatiles.

Keywords: Pluto; Charon

1. Introduction

The discovery of Pluto's moon Charon (Christy and Harrington, 1978) provided new opportunities to explore the smallest planet in our Solar System. From the orbital period and semimajor axis of Charon's orbit about Pluto, the mass of the binary system was determined (Beletic et al., 1989; Tholen and Buie, 1990). From the motions of Charon and Pluto about their barycenter, we establish the ratio of their masses and thus their individual masses, bulk densities, and rock-mass fractions. These parameters help us to understand the interior and history of each body. For example, McKinnon (1989) showed that Charon's density can be a clue to the origin of the binary system: a density greater than 1.8 $\mathrm{g\,cm^{-3}}$ implies a collisional origin for the system. The rock-mass fraction provides clues as to the formation of these bodies. It is an indicator of the cosmochemical abundances because bodies have different cosmochemical abundances due to the amount of carbon bonded with oxygen (in CO) or hydrogen (in CH_4) depending on whether they formed in a solar nebula or a planetary nebula.

In the past decade (as instrumentation has improved) there has been a flurry of activity to measure the wobble of Pluto about the Pluto/Charon barycenter. Five earlier determinations, whose results are summarized in Table 1, include three based upon HST WFPC data (Null et al., 1993; Null and Owen, 1996; Tholen and Buie, 1997) and two from ground-based observations (Young et al., 1994; Foust et al., 1997). Young et al. (1994) measured the motion of Pluto about the system's barycenter using ground-based imaging over 78% of an orbit and numerical PSF modeling to derive the individual centers of Pluto and Charon, and hence their motions. Foust et al. (1997) modeled center-of-light obser-

Table 1
Previous mass ratio solutions

Reference	Mass ratio
Null et al. (1993)	0.084 ± 0.015
Young et al. (1994)	0.157 ± 0.003
Null and Owen (1996)	0.124 ± 0.008
Tholen and Buie (1997)	0.110 ± 0.060
Foust et al. (1997)	0.117 ± 0.006

☆ Based on observations made with the NASA/ESA Hubble Space Telescope, obtained at the Space Telescope Science Institute, which is operated by the Association of Universities for Research in Astronomy, Inc., under NASA contract NAS 5-26555. These observations are associated with proposal #7494.

* Corresponding author.
E-mail address: colkin@alum.mit.edu (C.B. Olkin).

0019-1035/03/$ – see front matter
doi:10.1016/S0019-1035(03)00136-2

vations of the unresolved pair to determine the wobble about the barycenter.

Null et al. (1993) determined the motion of Pluto about the system barycenter using images of Pluto and Charon with only one available reference star. Therefore, the orientation of the field could be determined only from the barycentric ephemeris motion of Pluto–Charon. The second publication (Null and Owen, 1996) included additional WFPC data of Pluto and its satellite and had an improved characterization of the field distortion. Hence, the 1996 result supersedes their previous solution.

While not specifically designed as an astrometric study relative to a fixed coordinate system, the Tholen and Buie (1997) observations, nevertheless, yielded a value for the mass ratio. During most of these observations at least one star was visible in the field with Pluto and Charon. As part of their plate scale determination, the investigators combined their observed individual Pluto and Charon pixel positions with an assumed mass ratio to get an observed barycenter position. Using frames separated by hours, they determined an observed motion of the barycenter which was combined with the ephemeris motion to get a plate scale. To determine the mass ratio, the plate-scale fit was repeated for different assumed values of mass ratio until a solution with the smallest chi-squared was found.

2. Observations

We used the fine guidance sensor #3 with the F583W filter to carry out astrometry of Pluto, Charon, and a total of five reference stars on five appropriately chosen orbits of HST spanning 4.4 days. The capability of this instrument to carry out astrometry of this type at the level of accuracy required for this research has been amply demonstrated through its use in TRANS/POS mode observations of binary-star components relative to one another (Franz et al., 1998) and to local reference stars (Benedict et al., 2001).

We chose to observe Pluto near its stationary point to maximize the amount of time that Pluto, Charon, and the reference stars would remain in the field of the FGS (the pickle; see Fig. 1). More reference stars were available in the field of the March 1998 stationary point than for other opportunities. The combination of FGS #3 and the F583W filter has a well-calibrated optical field angle distortion (OFAD) correction (McArthur et al., 1997). For each observation, Pluto and Charon were placed at the center of the pickle where the TRANS mode transfer function is calibrated. One reference star was measured at the beginning and end of each visit to check for drift. We chose epochs of observation such that Pluto and Charon would be clearly resolvable on both interferometer axes while maintaining near uniform orbital phase coverage and maximizing the number of common reference stars.

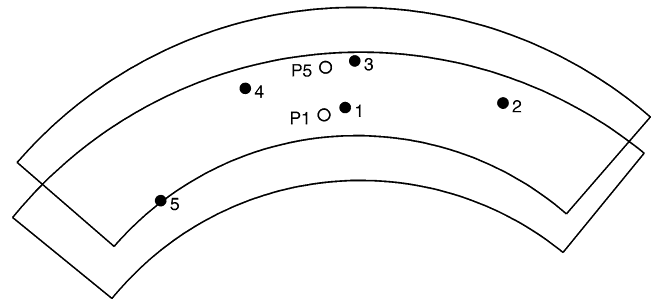

Fig. 1. The observed field. The Pluto–Charon binary is represented by an open circle and the reference stars by a filled circle. “P1” and “P5” indicate the position of the binary during the first and last HST visits. Also shown is the FGS pickle (or total field of view) for the first and last visit. Note that the Pluto–Charon binary is centered in the pickle and that we retained as many common reference stars as possible. The pickle is a quarter annulus at the outer perimeter of the HST focal plane with an inner radius of 10 arcmin and outer radius of 14 arcmin.

On each HST orbit, we observed four to five reference stars in POS mode to obtain their positions with milliarcsec precision in pickle coordinates (spacecraft-fixed coordinates). Unfortunately, even near Pluto’s stationary point, we could not observe all the same reference stars on all five visits owing to the motion of Pluto and the spacecraft orientation. Three of the reference stars were observed in all the spacecraft orbits, another reference star was common to all but the first visit, and yet another was common to the first two visits only. Table 2 gives the observed centers for Pluto, Charon and each of the reference stars on all of the visits (after the OFAD calibration was applied, see below). The units are pickle coordinates in arcsec.

3. Data reduction and analysis

The individual centers for Pluto and Charon were determined from TRANS mode observations. For each visit, 18–20 scans were coadded by cross correlation to reduce

Table 2
Measured photocentric positions of Pluto, Charon and the reference stars in FGS-X, Y coordinates

Visit	Pluto		Charon		Star 1		Star 2		Star 3		Star 4		Star 5	
	X	*Y*	*X*	*Y*	*X*	*Y*	*X*	*Y*	*X*	*Y*	*X*	*Y*	*X*	*Y*
1	2.5946	730.5566	2.9096	730.7230	−38.1236	740.2116	−332.7985	719.5553	–	–	144.5469	794.4769	322.5694	600.9017
2	2.5250	731.2603	2.9360	730.9740	−37.0894	729.5345	−331.2752	702.8461	−65.0281	814.0757	144.4290	787.5317	326.3706	597.6477
3	2.3956	731.0870	2.1112	730.7618	−25.2879	681.6778	−320.1825	664.4983	−50.4809	767.0752	158.0106	733.7825	–	–
4	1.9536	731.9629	1.5389	732.2329	−20.5406	669.4243	−315.4822	653.0314	−45.5085	754.8890	162.8954	721.0414	–	–
5	0.8107	734.1880	0.4662	734.9649	−16.0956	657.3599	−311.2926	646.0970	−39.5777	743.2428	168.2113	705.7740	–	–

noise. Because Pluto appears marginally resolved, a standard stellar transfer function could not be used in the analysis. Instead, a model for the Pluto transfer function was derived intrinsically from the Pluto–Charon data by subtracting the Charon component (modeled as a point source) and averaging all the Pluto-only transfer function data. The transfer-function fits of the TRANS-mode data provide positions for Pluto and Charon in the same pickle coordinates as the reference stars. The coadded transfer function and its fit from our first observation in X and Y pickle coordinates are shown in Fig. 2.

The OFAD calibration was applied to the pickle coordinates for the reference stars, Pluto, and Charon. The "Whipple" correction (Franz et al., 1998) was applied to the Pluto and Charon TRANS mode observations. After applying the calibrations, we have five sets of corrected positions for Pluto, Charon, and the reference stars with each set in its own spacecraft-fixed pickle coordinates. With the use of linear "plate constants" determined by least-squares solutions, we then transformed these corrected observation sets to a common reference frame, choosing visit 2 as our "standard plate." The RMS residuals for visits 1, 3, 4, and 5 transformed to visit 2 are 4 mas, 1 mas, 1 mas, and 6 mas, respectively.

Finally we transformed, by linear least-squares solutions, the five sets of Pluto and Charon coordinates from the "standard plate" reference frame to sky with the use of star positions measured at the US Naval Observatory Flagstaff Astrometric Scanning Transit Telescope (Stone et al., 1996). Table 3 contains the celestial coordinates of the reference stars as supplied by R.C. Stone (personal communication). The residuals for each star from this transformation are given in Table 4 (Fit #1). Unfortunately, the HST and USNO observations of the reference stars were not contemporaneous, and star 4 has a large residual. We, therefore, eliminated this star. The residuals from the improved transformation are also given in Table 4 (Fit #2).

Using Fit #2, we find the observed position of star #4 to be (J2000) RA = 16 h, 33 m, 19.8728 s and Dec = $-9^\circ\,34'\,24''.4569$ which is significantly discrepant from R.C. Stone's position in Table 3. Investigating this further we find positions for this star in both the USNO A2

Table 3
Astrometric reference stars

Star	RA (J2000)	σ(RA) (arcsec)	Dec (J2000)	σ(Dec) (arcsec)	V	#obs	Epoch of obs
1	16:33:07.221	0.022	−9:35:00.49	0.015	14.41	6	1999.516
2	16:32:47.256	0.049	−9:34:51.97	0.020	12.36	8	1999.513
3	16:33:06.024	0.039	−9:33:33.21	0.017	13.37	7	1999.513
4	16:33:19.873	0.042	−9:34:24.41	0.021	13.68	7	1999.513
5	16:33:30.566	0.032	−9:37:54.63	0.054	14.59	7	1999.513

Table 4
Residuals of sky-plane transformation

Star	Fit #1		Fit #2	
	x (mas)	y (mas)	x (mas)	y (mas)
1	−0.2	−8.7	1.5	−0.9
2	1.7	9.9	−0.4	0.2
3	−4.9	−18.8	−0.7	0.4
4	4.8	22.0	–	–
5	−1.4	−4.4	−0.4	0.2

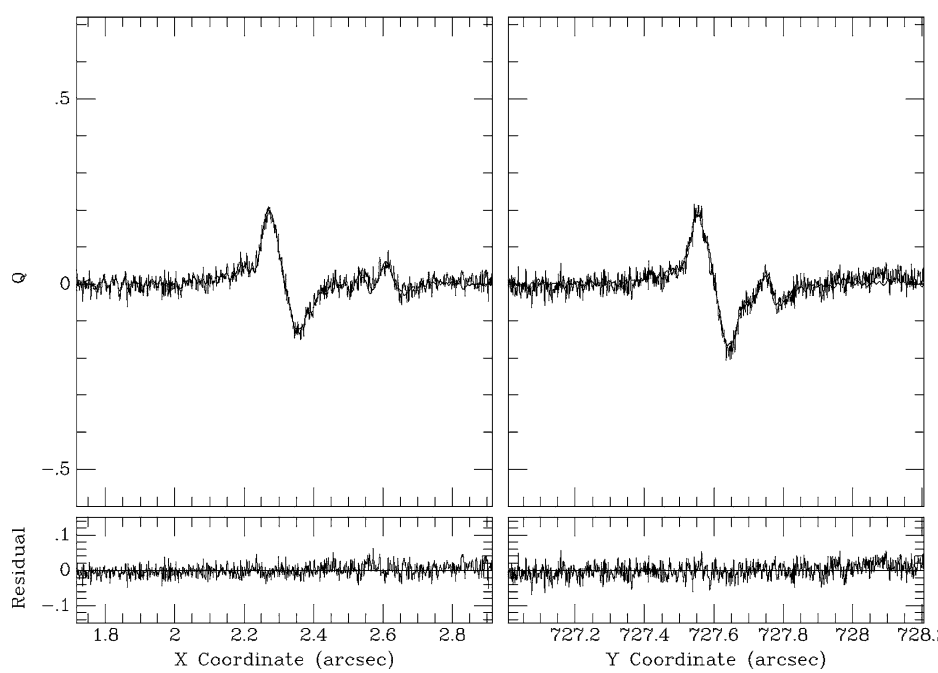

Fig. 2. Plot of the FGS transfer function (Q) in X (left) and in Y (right) for the first observation set. The fitted transfer function as a superposition of the individual transfer functions of Pluto and Charon is shown as a solid line with the residuals of the fit at the bottom. In both X and Y the larger peak is due to Pluto with the smaller peak being due to Charon.

and B1.0 catalogs (RA = 16 h, 33 m, 19.8647 s, Dec = $-9° 34' 24''.250$ and RA = 16 h, 33 m, 19.9027 s, Dec = $-9° 34' 24''.220$). These positions are even more discrepant. This lack of consensus in star #4's position could be a result of the star having multiple components of different colors, significant proper motion, and/or parallax. Whatever the cause, we do not know the position of star #4 adequately enough to include it in this analysis.

The resulting sky-plane positions of Pluto and Charon are given in Table 5. Rectangular coordinates of Charon relative to Pluto corresponding to these positions are illustrated in Fig. 3, fitted by an apparent binary orbit with the eccentricity held to zero and the period held to the known value of 6.3872464 days. The resulting semi-major axis, $a = 19850 \pm 190$ km, compares well with the value of $a = 19636 \pm 8$ km derived by Tholen and Buie (1997) using 60 WFPC1 measures over 72 orbits. Although this best-fitting orbit is not directly relevant to this investigation it does give an indication of the precision of the FGS TRANS measures used in this study.

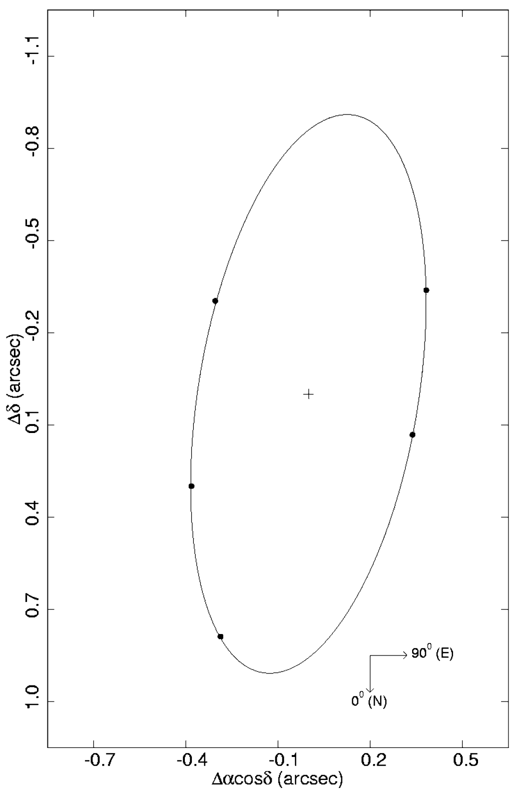

Fig. 3. Plot of the apparent orbit of Charon about Pluto. The points are measured relative positions transformed from FGS coordinates to equatorial. The line is the fitted apparent relative orbit with the eccentricity held to zero and the period to the known value of P = 6.3872464 days. While not directly relevant to this paper, this apparent orbit clearly demonstrates the precision of our differential measures. Note that the residual vectors are shown in the figure, but are too small to be seen.

4. The mass ratio

To derive the Charon–Pluto mass ratio (q), we first subtract the barycentric coordinates (given by JPL ephemeris DE405), computed at the topocentric position of HST, from the observed sky-plane positions of both Pluto and Charon, converting the RA difference to arcsec. The individual barycentric Charon and Pluto positions (x_c, y_c, x_p, y_p) are related to the mass ratio (q) in Eqs. (1). Note that we aligned x with Dec and y with RA. The zero-point terms on the right-hand side (x_0, y_0) allow for an offset of the ephemeris and our measured coordinates

$$x_p/(1+q) + x_c q/(1+q) = x_0,$$
$$y_p/(1+q) + y_c q/(1+q) = y_0. \quad (1)$$

We used least-squares fits to determine the mass ratio and zero-point terms. Three solutions are displayed in Table 6: (i) using only the x-data, (ii) using only the y-data, (iii) and using all data. There is agreement between the three solutions in all three fitted parameters (q, x_0, y_0). The RMS residual per degree of freedom has a range of 6–8 mas. While this would be large for a stellar binary system, it is not surprising owing to the additional complexities of the Pluto–Charon case.

We adopt a value of 0.122 ± 0.008 for the mass ratio of Charon to Pluto (our "all data" solution). Comparing this solution with previous reports in the literature (Table 1), we find consistency with all but the first two. As noted previously, the Null et al. (1993) result is superseded by the Null and Owen (1996) solution.

Next, consider the zero-point terms in Table 6. We find the barycenter of the Pluto/Charon system to be 68 ± 3 mas West and 42 ± 3 mas South of the barycentric position given by DE405. This large offset could be due to errors in the reference star network, an offset of Pluto from its ephemeris, or a combination of both. This is a potentially interesting

Table 5
Pluto/Charon equatorial positions (J2000)

Date (UT)	Pluto		Charon	
	RA	Dec	RA	Dec
1998 03 12 06:16:30.85	16:33:09.896	−09:35:14.10	16:33:09.919	−09:35:13.97
1998 03 12 19:09:52.68	16:33:09.894	−09:35:03.48	16:33:09.920	−09:35:03.82
1998 03 15 06:52:55.08	16:33:09.375	−09:34:13.65	16:33:09.354	−09:34:13.95
1998 03 15 23:00:52.93	16:33:09.091	−09:34:00.05	16:33:09.066	−09:33:59.75
1998 03 16 16:45:34.65	16:33:08.708	−09:33:44.93	16:33:08.689	−09:33:44.14

Table 6
Least-squares solutions

	Mass ratio	x_0 (mas)	y_0 (mas)	RMS residual (mas)
x-data only	0.114 ± 0.008	-43 ± 3	–	6
y-data only	0.133 ± 0.014	–	-68 ± 4	8
all data	0.122 ± 0.008	-42 ± 3	-68 ± 3	7

Table 7
Distance of Pluto from the system barycenter

Visit	Pluto from barycenter	
	x (arcsec)	y (arcsec)
1	0.014	0.037
2	−0.037	0.041
3	−0.033	−0.033
4	0.033	−0.041
5	0.086	−0.032

Table 8
Masses, densities and rock fractions

	Pluto		Charon	
Mass (10^{24} g)	13.12 ± 0.65		1.60 ± 0.12	
Radius (km)	1151 ± 6	1195 ± 5	593 ± 13	621 ± 21
Density (g cm^{-3})	2.05 ± 0.11	1.83 ± 0.09	1.83 ± 0.18	1.59 ± 0.20
Rock-mass fraction	0.77 ± 0.04	0.68 ± 0.04	0.68 ± 0.08	0.56 ± 0.12

side product of our work which may well deserve further, yet separate, investigation.

We have assumed implicitly that the derived positions for Pluto and Charon correspond to their physical centers. However, we are effectively measuring their photocenters. Since Charon appears to have little photometric variability with rotational phase (Buie et al., 1997), this distinction is not important. Pluto, on the other hand, has long been observed to vary in brightness with rotational phase (Walker and Hardie, 1955; Andersson and Fix, 1973; Tholen and Tedesco, 1994; Buie et al., 1997). This variability is the result of bright and dark patches on Pluto's surface and will change with rotational phase, sub-Earth latitude, and season as surface frost migrates due to sublimation and deposition. The current estimate of the center-of-light (COL) to center-of-body (COB) offset is mostly in declination (Foust et al., 1997). Such an offset could mask itself in the wobble of Pluto about the barycenter and, if significant, would be seen as a difference in mass ratio between the x- and y-data solutions or an increased error in the x solution, which is not the case.

The amplitude of this offset has been estimated to be ~ 5 mas, but is highly dependent on the Pluto map used. Since Pluto's albedo patterns likely vary with time and wavelength, the map would have to correspond to the correct epoch and wavelength. Using Eqs. (1), our mass ratio result, and the distances of Charon from Pluto corresponding to the positions given in Table 5, we can determine the (x, y) distance of Pluto from the system barycenter given in Table 7. Given the size of the offset of Pluto from the barycenter, we estimate the error contribution to the mass ratio from the COL to COB offset to be not more than 5–10% of the mass ratio.

Orbital phase is another effect that can offset the center of light from the geometric center. The orbital phase of Pluto was less than 2° shifting the photocenter less than 1 mas from the geometric center. This is below our detection level.

In Table 8, we present the masses, densities, and rock-mass fractions derived from our adopted mass ratio and assuming a system mass of $(14.72 \pm 0.72) \times 10^{24}$ g (Tholen and Buie, 1990). For each, Pluto and Charon, two different radii representing the full range of currently accepted values are presented. The lower value for Pluto's radius (1151 ± 6 km) is determined from mutual event data (Tholen and Buie, 1990) with the scale derived from the semimajor axis of Charon's orbit (Tholen and Buie, 1997). The upper value for Pluto's radius comes from analysis of a 1988 stellar occultation by Pluto (Millis et al., 1993). Different solutions for Pluto's solid surface radius exist depending on the interpretation of the "knee" in the occultation light curve. This value (1195 ± 5 km) is based on the assumption of a clear atmosphere.

There is also uncertainty in Charon's radius. The lower value (593 ± 13 km) comes from the same analysis as Pluto's lower limit. The larger value (621 ± 21 km) also comes from mutual event data (Young and Binzel, 1994) but with an assumption of limb darkening.

In no case do we find a Charon more dense than Pluto. Only with the smallest radii does Charon's density reach the value of 1.8 g cm^{-3}. For Charon densities greater than 1.8 g cm^{-3}, McKinnon (1989) found that Pluto and Charon had to have formed collisionally.

From these densities, a rock density of 3.0 g cm^{-3} and an ice density of 1.0 g cm^{-3}, we derive rock-mass fractions for both Pluto and Charon. The resulting rock-mass fraction for Pluto (0.68–0.77) is similar to that for Triton (0.7). The rock-mass fraction for Charon (0.56–0.68) indicates a larger ice component. Values of the rock-mass fraction greater than one half are difficult to explain with the current models for the outer solar nebula. Even with all the carbon in the nebula bound in CO (rather than methane), current models do not predict such rocky condensates from the outer solar nebula (Anders and Grevesse, 1989; Grevesse et al., 1991). The large rock-mass fractions for Pluto and Triton may be a result of catastrophic events in their history leading to a loss of volatiles (McKinnon et al., 1997). Such a catastrophic event could be the collisional origin of the Pluto–Charon binary.

From density and radius, interior models can be developed. McKinnon et al. (1997) present a model for Pluto with a radius of 1200 km and a density of 1.85 g cm^{-3} which corresponds very nicely to our findings. They found Pluto to be differentiated under these conditions and that smaller and more dense Pluto models had similar differentiated interiors.

5. Conclusions

Based upon astrometric measurements with HST fine guidance sensor #3, we find the mass ratio of Charon to Pluto to be 0.122 ± 0.008. It should be noted that this value is nearly equal to the average of the five previous determinations.

From our mass ratio, we find the density of Pluto (1.8–2.1 $\mathrm{g\,cm^{-3}}$) to be similar to Triton's ($2.05 \pm 0.03\ \mathrm{g\,cm^{-3}}$, Tyler et al., 1989). These bodies are rockier than expected by current models of the early solar nebula. With our measurement of the mass ratio, the uncertainties in the densities of Pluto and Charon no longer come from the mass ratio, but from the radii. The best way to improve this situation (in the near term) would be a well-observed stellar occultation. Definitive results may well have to await a spacecraft mission to Pluto.

Acknowledgments

We thank Barbara McArthur and G. Fritz Benedict of the University of Texas at Austin for their assistance with the POS data reduction. We also thank Ron Stone of the US Naval Observatory Flagstaff Station for providing measurements of our astrometric reference stars. Support for proposal #7494 was provided by NASA through a grant from the Space Telescope Science Institute, which is operated by the Association of Universities for Research in Astronomy, Inc., under NASA contract NAS 5-26555.

References

Anders, E., Grevesse, N., 1989. Abundances of the elements: meteoritic and solar. Geochim. Cosmochim. Acta 53, 197–214.

Andersson, L.E., Fix, J.D., 1973. Pluto: new photometry and a determination of the axis of rotation. Icarus 20, 279–283.

Benedict, G.F., McArthur, B.E., Franz, O.G., Wasserman, L.H., Henry, T.J., Takato, T., Strateva, I.V., Crawford, J.L., Ianna, P.A., McCarthy, D.W., Nelan, E., Jefferys, W.H., vanAltena, W., Shelus, P.J., Hemenway, P.D., Duncombe, R.L., Story, D., Whipple, A.L., Bradley, A.J., Fredrick, L.W., 2001. Precise masses for Wolf 1062 AB from Hubble Space Telescope interferometric astrometry and McDonald Observatory radial velocities. Astron. J. 121, 1607–1613.

Beletic, J.W., Goody, R.M., Tholen, D.J., 1989. Orbital elements of Charon from speckle interferometry. Icarus 79, 38–46.

Buie, M.W., Tholen, D.J., Wasserman, L.H., 1997. Separate lightcurves of Pluto and Charon. Icarus 125, 233–244.

Christy, J.W., Harrington, R.S., 1978. The satellite of Pluto. Astron. J. 83, 1005–1008.

Foust, J.A., Elliot, J.L., Olkin, C.B., McDonald, S.W., Dunham, E.W., Stone, R.P.S., McDonald, J.S., Stone, R.C., 1997. Determination of the Charon/Pluto mass ratio from center-of-light astrometry. Icarus 126, 362–372.

Franz, O.G., Henry, T.J., Wasserman, L.H., Benedict, G.F., Ianna, P.A., Kirkpatrick, J.D., McCarthy Jr., D.W., Bradley, A.J., Duncombe, R.L., Fredrick, L.W., Hemenway, P.D., Jefferys, W.H., McArthur, B.E., Nelan, E.P., Shelus, P.J., Story, D.B., van Altena, W.F., Whipple, A.L., 1998. The first definitive binary orbit determined with the Hubble Space Telescope fine guidance sensors: Wold 1062 (Gliese 748). Astron. J. 116, 1432–1439.

Grevesse, N., Lambert, D.L., Sauval, A.J., vanDishoeck, E.F., Farmer, C.B., Norton, R.H., 1991. Vibration-rotation bands of CH in the solar infrared spectrum and the solar carbon abundance. Astron. Astrophys. 242, 488–495.

McArthur, B., Benedict, G.F., Jefferys, W.H., Nelan, E., 1997. Maintaining the FGS3 optical field angle distortion calibration. In: Castertano, S., Jedrzejewski, R., Keyes, T., Stevens, M. (Eds.), Proc. of the 1997 HST Calibration Workshop With a New Generation of Instruments, pp. 472–480.

McKinnon, W.B., 1989. On the origin of the Pluto–Charon binary. Astrophys. J. 344, L41–L44.

McKinnon, W.B., Simonelli, D.P., Schubert, G., 1997. Composition, internal structure and thermal evolution of Pluto and Charon. In: Stern, S.A., Tholen, D.J. (Eds.), Pluto and Charon. Univ. Arizona Press, Tiscon, AZ, pp. 295–343.

Millis, R.L., Wasserman, L.H., Franz, O.G., Nye, R.A., Elliot, J.L., Dunham, E.W., Bosh, A.S., Young, L.A., Slivan, S.M., Gilmore, A.C., Kilmartin, P.M., Allen, W.H., Watson, R.D., Dieters, S.W., Hill, K.M., Giles, A.B., Blow, G., Priestley, J., Kissling, W.M., Walker, W.S.G., Marino, B.F., Dix, D.G., Page, A.A., Ross, J.E., Avey, H.P., Hickey, D., Kennedy, H.D., Mottram, K.A., Moyland, G., Murphy, T., Dahn, C.C., Klemola, A.R., 1993. Pluto's radius and atmosphere: results from the entire 9 June 1988 occultation data set. Icarus 105, 282–297.

Null, G.W., Owen Jr., W.M., 1996. Charon/Pluto mass ratio obtained with HST CCD observations in 1991 and 1993. Astron. J. 111, 1368–1381.

Null, G.W., Owen, W.M., Synnott, S.P., 1993. Mass and densities of Pluto and Charon. Astron. J. 105, 2319–2335.

Stone, R.C., Monet, D.G., Monet, A.K.B., Walker, R.L., Ables, H.A., Bird, A.R., Harris, F.H., 1996. The Flagstaff Astrometric Scanning Transit Telescope (FASTT) and star positions determined in the extragalactic reference frame. Astron. J. 111, 1721–1742.

Tholen, D.J., Buie, M.W., 1990. Further analysis of the Pluto–Charon mutual event observations—1990. Bull. Am. Astron. Soc. 22, 1129.

Tholen, D.J., Buie, M.W., 1997. The orbit of Charon I. New Hubble Space Telescope observations. Icarus 125, 245–260.

Tholen, D.J., Tedesco, E.F., 1994. Pluto's lightcurve: results from four oppositions. Icarus 108, 200–204.

Tyler, G.L., Sweetnam, D.N., Anderson, J.D., Borutzki, S.E., Campbell, J.K., Kursinski, E.R., Levy, G.S., Lindal, G.F., Lyons, J.R., Wood, G.E., 1989. Voyager radio science observations of Neptune and Triton. Science 246, 1466–1473.

Walker, M.F., Hardie, R., 1955. A photometric determination of the rotational period of Pluto. Publ. Astron. Soc. Pacific 67, 224–231.

Young, E.F., Binzel, R.P., 1994. A new determination of radii and limb parameters for Pluto and Charon from mutual event lightcurves. Icarus 108, 219–224.

Young, L.A., Olkin, C.B., Elliot, J.L., Tholen, D.J., Buie, M.W., 1994. The Charon–Pluto mass ratio from MKO astrometry. Icarus 108, 186–199.